Correspondence to:
K. M. Straub,
kmstraub@tulane.edu

Influence of sediment cohesion on deltaic shoreline dynamics and bulk sediment retention: A laboratory study

Kyle M. Straub[1], Qi Li[1], and W. Matthew Benson[1]

[1]Department of Earth and Environmental Sciences, Tulane University of Louisiana, New Orleans, Louisiana, USA

Abstract While boundary and forcing conditions influence the average location of a shoreline in deltaic systems, internal morphodynamics can drive high-magnitude deviations from the long-term trend. Here we explore the role of sediment cohesion on these morphodynamics using physical experiments. Specifically, we explore the role of sediment cohesion on the scales of autogenic shoreline transgressions and regressions. Results indicate that sediment cohesion enhances the time and space scales associated with autogenic cycles of channel formation, elongation, and abandonment. In systems with high sediment cohesion, this cycle can drive shoreline transgressions that produce flooding surfaces in the resulting stratigraphy which could be confused with surfaces produced by increases in sea level rise or subsidence rates. Enhanced channelization resulting from sediment cohesion also increases the pumping of fine-grained sediment into the marine realm, where it can bypass the delta foreset, thus decreasing total delta sediment retention rate.

1. Introduction

A suite of recent studies demonstrate the importance of sediment cohesion on the morphology and dynamics of channelized environments [*Peakall et al.*, 2007; *Hoyal and Sheets*, 2009; *Martin et al.*, 2009b; *Edmonds and Slingerland*, 2010]. The cohesion of sediment is influenced by many factors, including the diameter, mineralogy, and compaction history of sediment, and the density and type of riparian vegetation [*Davies and Gibling*, 2011; *Grabowski et al.*, 2011]. Focusing on deltas, results from numerical and laboratory experiments demonstrate that sediment cohesion can influence morphology as much as wave or tide environment or the quantity of sediment entering a system. Specifically, increasing sediment cohesion appears to increase the rugosity of deltaic shorelines and produce more complex floodplains [*Hoyal and Sheets*, 2009; *Edmonds and Slingerland*, 2010].

The majority of experimental studies on deltas and sediment cohesion focus on their morphology in settings with constant sea level, with some notable exceptions [*Martin et al.*, 2009b]. We are interested in the influence of sediment cohesion on deltaic dynamics and resulting stratigraphy over basin-filling time scales where deltas experience the creation of accommodation through changes in absolute sea level and subsidence. A rich body of work details how changing the ratio of accommodation creation to deltaic sediment supply influences the movement of shorelines and the production of stratigraphic architecture [*Van Wagoner et al.*, 1990; *Muto and Steel*, 1997]. Many of these models assume 100% retention of sediment entering a delta, with the partitioning between delta topset, foreset, and bottomset dictated by geometric constraints [*Swenson et al.*, 2000]. However, it is also well known that boundary conditions, including waves and tides, influence bulk deltaic sediment retention rates (f_{SR}) [*Syvitski*, 2005]. However, outside of grain size [*Orton and Reading*, 1993; *Kostic et al.*, 2002], the influence of sediment properties including cohesion on f_{SR} in deltas is not well known. Several studies show a link between vegetation, often linked to sediment cohesion, and the trapping of fine-grained sediments on delta tops [*Gacia et al.*, 1999; *Li and Yang*, 2009; *Day et al.*, 2011], while others have found a more complicated relationship between vegetation and trapping efficiency [*Ortiz et al.*, 2013; *Nardin and Edmonds*, 2014]. When observed, enhanced sediment retention is generally linked to the drag imparted on sediment-laden overbanking flow from the stalks of vegetation. As such, the actual role of sediment cohesion on the trapping of sediment in deltas is not well known. This question has implications for the inversion of the stratigraphic record for paleosediment supply and the modeling of delta growth for ongoing and planned delta restoration projects [*Kim et al.*, 2009].

Table 1. Data Defining Boundary and Forcing Conditions of Three Experimental Stages and Variables Defining System Morphology and Deposit Properties[a]

Experiment	Experiment Run Time (h)	g Polymer per kg Sediment	Q_w (m³/s)	Q_s (kg/s)	r (mm/h)	S_T (1/1)	S_F (1/1)	ϕ (1/1)	D_{50} (μm)	H_c (mm)	L_b (m)
TDB-12 stage 0a—strongly cohesive	(—)127–0	1.47	1.72×10^{-4}	2.65×10^{-4}	0	2.2×10^{-2}	6.0×10^{-1}	N/A	N/A	N/A	N/A
TDB-12 stage 1—strongly cohesive	0–351	1.47	1.72×10^{-4}	2.65×10^{-4}	0.25	2.2×10^{-2}	5.7×10^{-1}	0.53[b]	N/A	N/A	N/A
TDB-12 stage 0b—strongly cohesive	351–385	1.47	1.72×10^{-4}	3.91×10^{-4}	0	2.4×10^{-2}	5.7×10^{-1}	N/A	N/A	N/A	N/A
TDB-12 stage 2—strongly cohesive	**385–1285**	**1.47**	$\mathbf{1.72\times10^{-4}}$	$\mathbf{3.91\times10^{-4}}$	**0.25**	$\mathbf{2.1\times10^{-2}}$	$\mathbf{5.8\times10^{-1}}$	0.53[b]	N/A	12.2	0.58
TDB-13 stage 0—noncohesive	(—)75–0	0	1.72×10^{-4}	3.91×10^{-4}	0	1.9×10^{-2}	5.0×10^{-1}	N/A	N/A	N/A	N/A
TDB-13 stage 1—noncohesive	**0–300**	**0**	$\mathbf{1.72\times10^{-4}}$	$\mathbf{3.91\times10^{-4}}$	**0.25**	$\mathbf{1.9\times10^{-2}}$	$\mathbf{5.6\times10^{-1}}$	0.40	83	2.3	0.12
TDB-13 stage 2—weakly cohesive	**300–700**	**0.73**	$\mathbf{1.72\times10^{-4}}$	$\mathbf{3.91\times10^{-4}}$	**0.25**	$\mathbf{2.2\times10^{-2}}$	$\mathbf{5.5\times10^{-1}}$	0.45	70	7.0	0.32

[a]The key stages discussed in the manuscript are in bold. Information on other stages is given for completeness as they would be necessary to reproduce modeling results.
[b]Measurement made from an experiment with identical polymer concentration, Q_w, Q_s, and r as TDB-12 stage 2.

While the influence of allogenic forcings (sea level, subsidence, and sediment supply) on the dynamics of shorelines is well studied, less is known about the role of internal (autogenic) processes in driving shoreline dynamics and their resulting stratigraphic products. Recent laboratory and numerical experiments utilizing noncohesive sediment have identified a link between autogenic storage and release of sediment and shoreline dynamics in alluvial fans and deltas [*Kim and Jerolmack*, 2008; *Nicholas et al.*, 2009; *Van Dijk et al.*, 2009; *Hamilton et al.*, 2013]. This storage and release has been linked to a commonly discussed autogenic cycle of channel initiation, extension, avulsion, and incision which initiates a new channel. However, in these experiments the difference in observed shoreline locations to those predicted from steady state models with no effects of autogenic processes was small and generally occurred over shorter time scales than collection of topographic scans making linkage of specific surface processes to their stratigraphic products difficult [*Kim and Jerolmack*, 2008; *Hamilton et al.*, 2013]. Further, whether the autogenic mechanism responsible for storage and release of sediment in these noncohesive experiments is important for more cohesive systems is yet to be explored. Here we examine the following two problems detailed above: (1) How does sediment cohesion influence the bulk retention of sediment in deltas and (2) how does sediment cohesion influence the time and space scales of autogenic shoreline dynamics and their stratigraphic products.

2. Experimental Methods

To examine the influence of sediment cohesion on sediment retention and the dynamics of deltaic shorelines, we performed experiments in the Delta Basin at Tulane University. As outlined in a review by *Paola et al.* [2009], reduced-scale physical experiments produce spatial structure and kinematics that, although imperfect, compare well with natural systems despite differences of spatial and temporal scales, material properties, and number of active processes. As such, we make no formal attempt to upscale our experiments to field scale but rather treat them as small systems of and to themselves.

We compare three experimental stages which share identical forcing conditions with the exception of the cohesion of sediment entering the basin (Table 1). Accommodation is created at a constant rate in all experiments by increasing ocean level utilizing a motorized weir that is in hydraulic communication with the basin. The computer-controlled ocean level rise rate (r) and input water (Q_w) and sediment discharge (Q_s) allowed the shoreline to be maintained at an approximately constant location through the course of the experiments but with superimposed fluctuations associated with autogenic processes. The input sediment mixture was designed to mimic earlier experimental work [*Hoyal and Sheets*, 2009] and had a broad particle size distribution, ranging from 1 to 1000 μm with a mean of 67 μm and was dominantly quartz. The sole difference in forcing conditions between the three experimental stages was the quantity of a polymer added to the input sediment. The enhanced cohesion provided by the polymer (New Drill Plus distributed by Baker Hughes Inc.) acts as a general proxy for the effect of vegetation and dewatered clays, which enables the formation of deltas with strong channelization at subcritical Froude numbers.
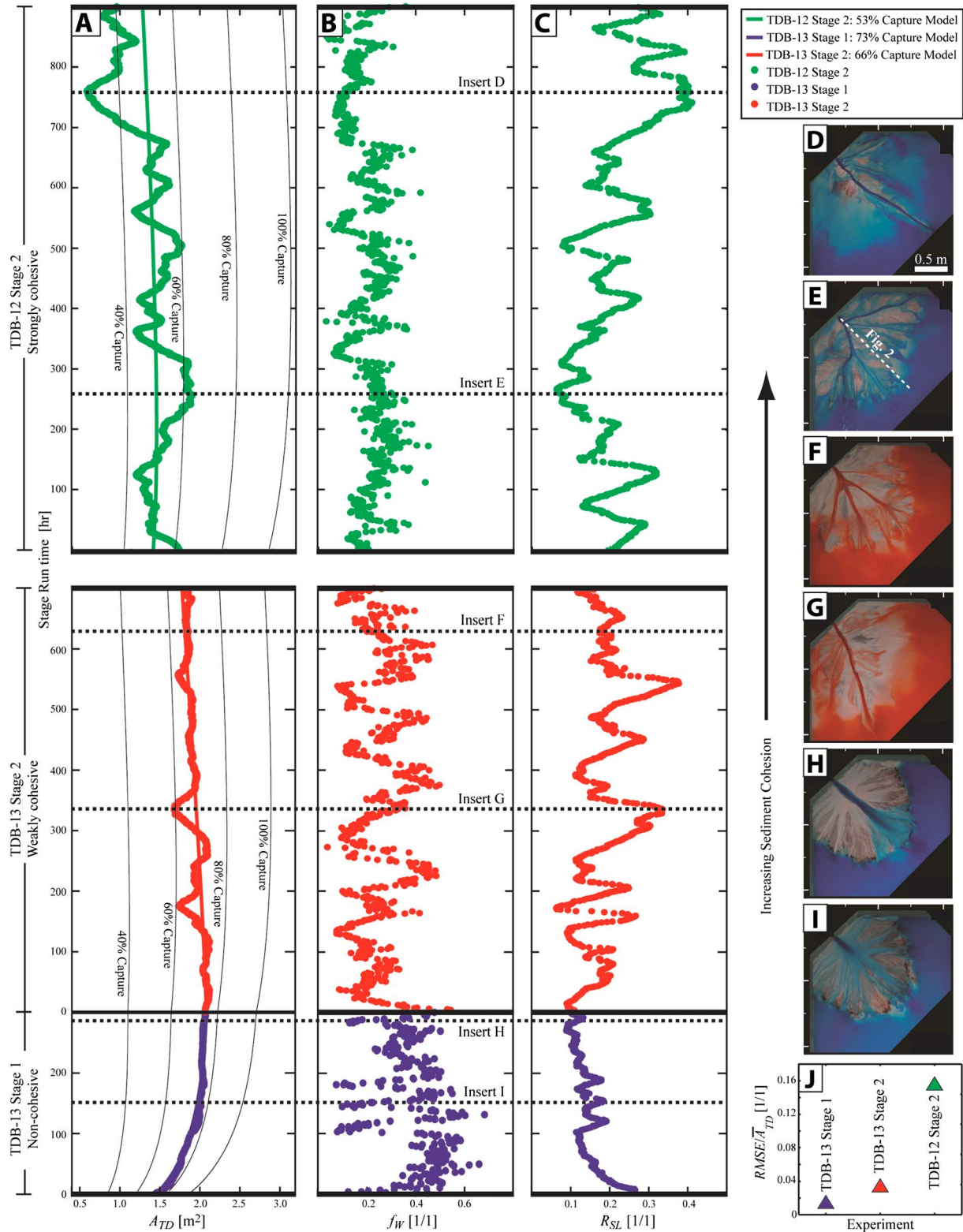
Figure 1. Evolution of terrestrial delta area and autogenic surface morphodynamics defined by experimental topography and overhead images of delta top with comparison to model results. (a) Time series of A_{TD} for the three experimental stages with comparison to numerical model results that minimize RMSE between model and data. (b) Time series of f_W for three stages. (c) Time series of R_{SL} for three stages. (d–i) Photos of experimental surface at time periods indicated by dashed lines. (j) Comparison of optimized RMSE normalized by $\overline{A}_{TD}$ between model and data for the three experimental stages.

The three experimental stages were performed over the course of two experiments. Experiment TDB-13 began with the progradation of a delta into a shallow ocean with constant ocean level for 75 h. This was followed by 300 h of run time and aggradation promoted through accommodation generation from base level rise. Input sediment during this stage (TDB-13-S1) had no added polymer. Immediately following, a second weakly cohesive stage (TDB-13-S2) was run for 700 h. This stage included 40 g of dry granular polymer per 54 kg of sediment and had the same base level rise rate as the noncohesive stage. A strongly cohesive stage was conducted as part of experiment TDB-12. This experiment also began with the progradation of a delta into an ocean of fixed depth, followed by aggradation drive by base level rise. Unfortunately, input Q_s during this initial aggradation was below our target rate. Following a brief pause in base level rise and adjustment of Q_s the main phase of this experiment began. This stage ran for 900 h with the same Q_w, Q_s, and ocean level rise rate as TDB-13 but with 80 g of polymer added per 54 kg of sediment (for details on experimental parameters see Table 1). While slight differences in initial ocean level and delta size exist between stages, the duration of each stage was sufficient to generate tens of channel depths worth of stratigraphy, thus reducing the importance of initial conditions on the bulk trends discussed below.

Topography was monitored with a 3-D laser scanner, resulting in digital elevation models (DEMs) with a 5 mm horizontal grid in the down and cross-basin directions, respectively, and < 1 mm of vertical resolution for terrestrial regions and areas with water depths < 50 mm. Topographic scans were collected once an hour for the duration of each experiment and shared the same datum as our ocean control system. This temporal and spatial resolution was sufficient to capture the mesoscale morphodynamics of the systems (e.g., channel and lobe avulsions). Following each, stage ocean water was cycled with clear water, which allowed average foreset slopes to be calculated from overhead photos and spot measurements of topography. Finally, we collected digital images of the active delta top every 15 min with input water dyed blue, which aid our characterization of morphodynamics.

3. Results

To examine the role of cohesion on deltaic sediment retention and shoreline dynamics we examine the evolution of terrestrial delta area (A_{TD}) in each experimental stage (Figure 1a). This is done by calculating the area of the delta above the elevation of the ocean surface for each DEM. Assuming a delta constructed of a topset and foreset with fixed slopes, S_T and S_F, respectively, delta growth theory suggests that given Q_s and positive r deltas will grow until reaching a maximum A_{TD} and then gradually loss A_{TD} [*Muto*, 2001; *Parker et al.*, 2008]. The eventual loss of A_{TD} is due to the ever increasing sediment demand of the growing foreset. After the initial stage with no ocean level rise, the noncohesive stage (TDB-13-S1) follows a relatively smooth trend of increasing A_{TD}. The moderately cohesive stage (TDB-13-S2), constructed on top of the noncohesive stage, was characterized by a long-term gradual decrease in A_{TD} with superimposed fluctuations away from this trend. The strongly cohesive stage (TDB-12) was characterized by a long-term gradual decrease in A_{TD} but with larger and longer fluctuations from the mean trend than the other stages.

Fluctuations in A_{TD} from the long-term trends were linked with phases of the autogenic channel cycle [*Hoyal and Sheets*, 2009]. We quantify this by tracking the fraction of the delta top covered by active flow (f_w) and the roughness of the shoreline (R_{SL}) each hour (Figures 1b and 1c). f_w is computed from wet/dry maps of experimental surfaces generated from overhead photos captured every 0.25 h [*Tal et al.*, 2012]. We quantify R_{SL} with the coefficient of variation for distances measured from points defining the shoreline to the basin entrance

$$R_{SL} = \sqrt{\frac{1}{N}\sum_{i=1}^{N}\left(\frac{r_i - \bar{r}}{\bar{r}}\right)^2} \tag{1}$$

where N is the total number of points defining the shoreline, r_i are the individual distance measurements, and $\bar{r}$ is the mean distance from basin entrance to shoreline for that run hour. Large values of R_{SL} thus indicate strong variability in the distance from the shoreline to basin inlet when normalized by the mean distance. These measurements reveal that periods with local maxima in A_{TD} are associated with distributed flow on delta tops following large avulsions and relatively smooth shorelines (Figures 1c, 1d, and 1g), while local minima in A_{TD} occur when shorelines are rough and follow long periods during which flow collapsed into single deep channels that effectively transferred sediment past the delta top (Figures 1b, 1e, and 1f).
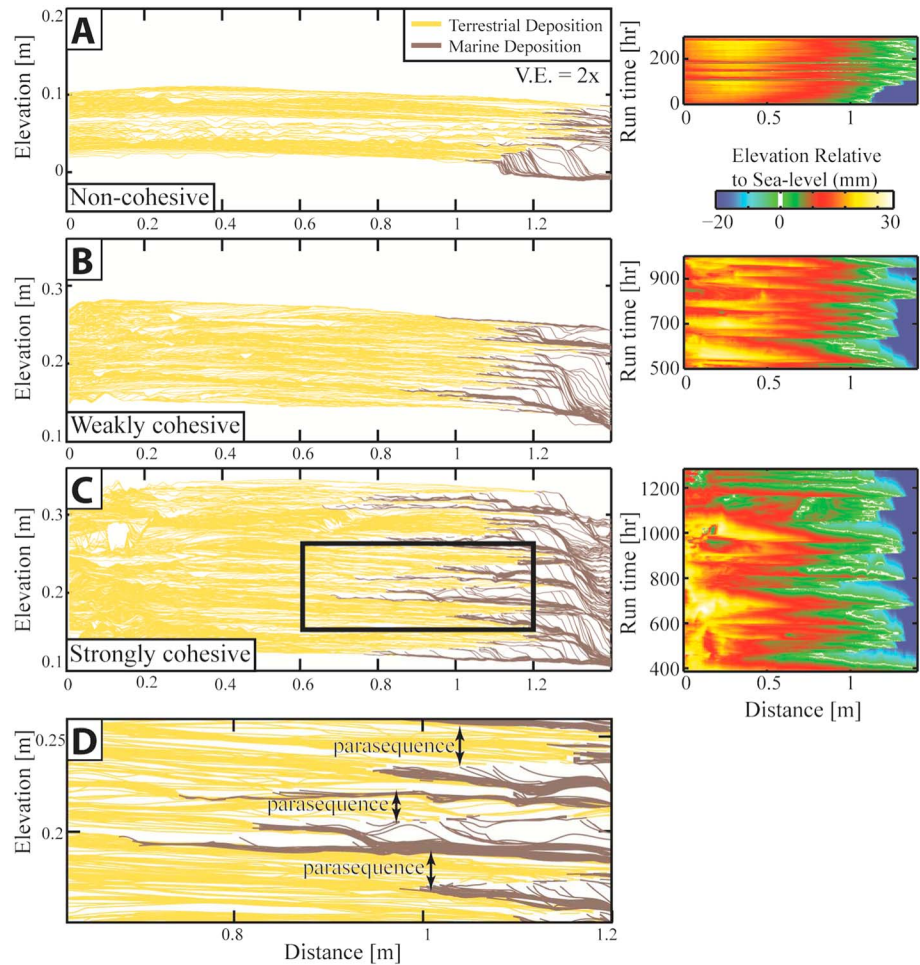
Figure 2. Data defining final deposit architecture and movement of shoreline for the three experimental stages along the dip transect labeled in Figure 1: (a) noncohesive, (b) moderately cohesive, and (c) strongly cohesive. Panels on the left are synthetic stratigraphic panels of the final deposit architecture colored by environment of deposition. Panels on the right are time-space matrixes of elevation relative to sea level. (d) Blowup of strongly cohesive stratigraphy from region outlined in box with example parasequences labeled.

To quantify the magnitude of the observed effects of autogenic process fluctuations in A_{TD} and f_{SR} we compare our A_{TD} time series to a model of delta growth that lacks autogenics [*Swenson et al.*, 2000]. This model calculates A_{TD} for a radial delta assuming sediment conservation for inputs of Q_s, deposit porosity (ϕ), S_T, S_F, and r. The transition in slope from S_T to S_F occurs at the shoreline where the delta elevation is equal to the ocean surface elevation. We began our modeling by assuming 100% retention of input sediment in the deltaic deposit and with values of ϕ, S_T, and S_F, measured from the DEMs or resulting deposit. This model results in predictions of A_{TD} that are much in excess of our observations (Figure 1a). The mismatch between model and data can likely be explained by the presence of a thick, flat, and fine-grained prodelta deposit observed beyond the delta foreset at the conclusion of each experiment, suggesting some sediment bypassed the delta. This is similar to previous observations made from experiments that used this sediment mixture [*Hoyal and Sheets*, 2009]. As such, we constructed additional models in which we augmented the sediment fraction necessary to conserve mass by simply multiplying our input Q_s by f_{SR}. For each experimental stage we determined the f_{SR} that minimizes the root-mean-square error (RMSE) normalized by mean delta area ($\overline{A}_{TD}$) of a stage. This method produces model time series that closely mimic the long-term trend of A_{TD} in each experimental stage. The key observations made from this analysis are as follows: (1) The f_{SR} that optimizes the fit between model and data decreases as sediment cohesion increases (Figure 1a), and (2) the normalized error of the optimized fits increases as sediment cohesion increases (Figure 1j), indicating larger autogenic fluctuations from the mean trend as sediment cohesion increases.
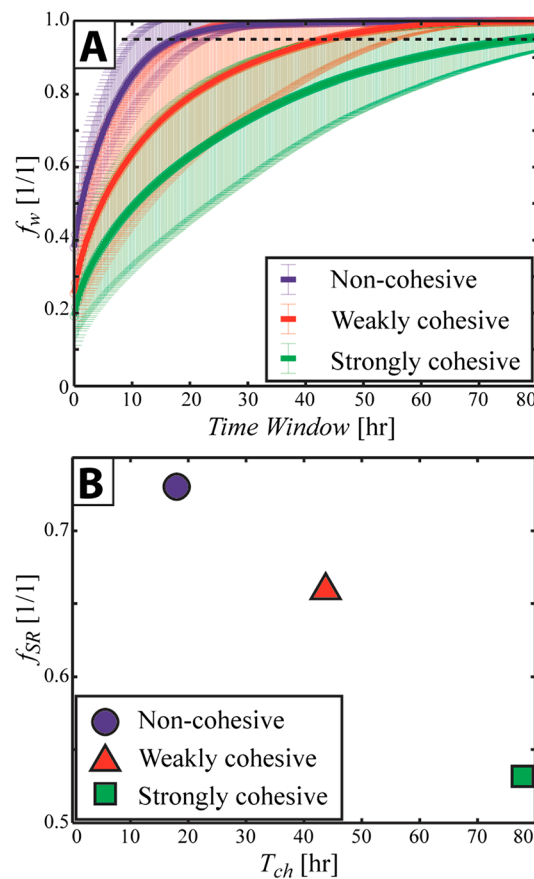
Figure 3. Data defining channel mobility and its implication on deltaic sediment retention. (a) Measurements of the increase in wet fraction on the fluvial surface as a function of time, used to estimate T_{ch}. Thick dashed lines represent time associated with wet fraction curve reaching 95% in each experiment. Error bars represent geometric standard deviation of each measurement. (b) Data defining relationship between T_{ch} and f_w in each experiment.

Utilizing the DEMs, we construct dip panels of synthetic stratigraphy from the entrance channel past the shoreline for each experiment (Figure 2). The synthetic stratigraphy is generated from stacked delta top profiles with topography clipped to account for sediment removed during erosion [*Martin et al.*, 2009a]. Using the coregistered ocean level control, we separate portions of the stratigraphy deposited in the terrestrial and marine realms. One key observation from these panels is the increase in scale of parasequences with an increase in sediment cohesion. Here parasequence is defined as a relatively conformable succession of genetically related strata bounded by marine flooding surfaces [*Van Wagoner et al.*, 1990] (Figure 2d). These parasequences formed autogenically, initiating with shoreline transgression due to flow abandonment on one part of the delta coupled with pseudosubsidence, followed later by deposition and shoreline regression due to flow reoccupation. In the noncohesive stage, where measurements of channel depth rarely surpassed 2.3 mm, flooding surfaces did not extend upstream of the model-projected shoreline by more than 85 mm. In contrast, in the strongly cohesive stage, where channel depths rarely surpassed 12.2 mm, flooding surfaces sometimes extended 425 mm upstream of the model-projected shoreline. Interestingly, the upstream extent of flooding surfaces in the three experimental stages, relative to the model-projected shoreline, appears to scale with the backwater length (L_B) of each system. L_B scales with the downstream extend of a reach in which the mean elevation of the bed of a channel descends below the ocean surface elevation and can be estimated as $L_B \sim H_c/S_T$ [*Parker*, 2004] (Table 1). Recent studies highlight the importance of L_B in sediment transport and morphodynamics [*Jerolmack*, 2009; *Nittrouer et al.*, 2012]. In the three experimental stages the upstream extend of the flooding surfaces, relative to our model predictions that lacked autogenics, ranged between 69 and 73% of L_B. In addition, the thickness of the parasequence deposits increases with cohesion in our experiments.

Sediment cohesion has been linked to strengthening of channel banks and reduction of channel mobility in previous studies [*Hoyal and Sheets*, 2009; *Caldwell and Edmonds*, 2014]. We quantify channel mobility in our experiments by measuring a channel time scale (T_{ch}), defined in previous studies as the time necessary for flow to visit 95% of a delta top [*Cazanacli et al.*, 2002; *Wickert et al.*, 2013]. Measuring T_{ch} is accomplished by monitoring the increase in the fraction of each delta visited at least once by flow for 80 h windows, starting every 0.25 h of run time. The resulting f_w curves are ensemble averaged to produce one representative curve for each stage (Figure 3a). Estimates of T_{ch} indicate a decrease in channel mobility as sediment cohesion increases. This result is consistent with the work of *Caldwell and Edmonds* [2014] who found a reduction in T_{ch} with sediment cohesion in numerical experiments. This decrease in channel mobility is also associated with a decrease in f_{SR} indicating that the less mobile a system is, the lower the deltaic sediment retention (Figure 3b). The wet/dry maps can also be used to quantify the degree of channelization in each stage. The value of f_w at time zero in Figure 3a represents the average fraction of a delta occupied by flow during a stage at any instant in time. We note that $f_{w,T=0}$ is greatest for the noncohesive stage and decreases with

increasing sediment cohesion, indicating flow collapse into fewer but deeper channels with increasing sediment cohesion.

4. Discussion

A major finding of this study is an inverse correlation between sediment cohesion and bulk deltaic sediment retention. In field scale systems, a primary control on sediment cohesion is the quantity and type of riparian vegetation, which in prior studies has been linked to enhanced sediment retention [*Li and Yang*, 2009; *Day et al.*, 2011]. These earlier studies have linked enhanced sediment retention to drag imparted on sediment-laden overbanking flow. This drag decreases flow velocities, thus decreasing the advection length scales of particles-exiting channels. Some recent studies, however, have highlighted that vegetation might in some cases reduce sediment-trapping efficiency [*Ortiz et al.*, 2013; *Nardin and Edmonds*, 2014]. In particular, results from the numerical experiments of *Nardin and Edmonds* [2014] suggest that sediment-laden flow in deltas might avoid vegetated overbank regions in favor of channels due to the surface roughness that comes with vegetation. While the experiments described here do not include any vegetation, they suggest that sediment cohesion provided by the roots of vegetation might enhance channelization and increase the life span of channels. Increasing sediment cohesion resulted in fewer, deeper channels that were more effective at advecting fine particles past the delta foreset. These effects, coupled to the processes suggested by *Nardin and Edmonds* [2014], likely aid the pumping of fine particles in channels to the marine. The loss of the fine load to the prodelta also suggests that cohesion might help coarsen a deltaic deposit, given two systems with identical input particle distributions but different cohesions. This effect was observed in the two experimental stages where the mean deposit particle size was measured (Table 1). Our results then raise the question, What control does vegetation has on deltaic sediment retention? Answering this question is outside the scope of this study, but our results do suggest that enhanced deposition due to drag imparted by the stalks of vegetation has to be balanced against a reduction in channel mobility which allows channels to act as conveyor belts for fine sediment to the deeper marine environment.

The experiments detailed here demonstrate how sediment cohesion can aid the formation of parasequences with lateral extents that scale with L_B. Given that L_B in some large deltaic systems can be in excess of 100 km [*Jerolmack*, 2009; *Nittrouer et al.*, 2012], this finding highlights the difficulty in separating parasequences resulting from autogenic processes and those resulting from allogenic forcings [*Van Wagoner et al.*, 1990]. However, we do note that no systematic up-section change is seen in the landward extent of parasequence flooding surfaces within a given experimental stage. This suggests that interpretation of stratigraphic architecture for allogenic forcings should be limited to the parasequence set scale or higher.

Finally, our stratigraphic and morphodynamic observations have implications for delta restoration projects. The increase in the lateral extent of flooding surfaces and longer channel time scales with increasing sediment cohesion suggests that given relative sea level rise, more cohesive deltas are less capable of visiting all locations and effectively distributing their sediment during a given time frame. As a result, large cohesive deltas (e.g., Mississippi River) may be the most vulnerable to flooding compared with their less cohesive cousins (e.g., Yellow River).

5. Summary

Motivated by previous studies that examine the influence of cohesion on deltaic morphology and dynamics over short time scales [*Hoyal and Sheets*, 2009; *Edmonds and Slingerland*, 2010], this paper presents results from a suite of experiments where sediment cohesion was varied for long time scale experiments where generation of accommodation through pseudosubsidence is important. The main results are summarized as follows.

1. Estimates of deltaic sediment retention made through a comparison of our experiments to a geometric model suggest that retention inversely scales with sediment cohesion, when all other parameters are held constant. This results form a decrease in channel mobility and an increase in channelization which promotes the pumping of fine-grained sediment to the marine. These results suggest a complex relationship between vegetation and sediment retention due to the competing influence of drag on sediment-laden flow from the stems of vegetation and the increase in pumping of fines to the marine from cohesion.

2. As sediment cohesion increased in our experiments, the time and space scales of autogenic processes increased. This resulted in transgressions and regressions that increased in magnitude as sediment cohesion increased due to long-term accommodation generation in the experiments. These shoreline dynamics resulted in stratigraphic architecture at the parasequence scale which could be mistaken for products of allogenic forcings.

References

Caldwell, R. L., and D. A. Edmonds (2014), The effects of sediment properties on deltaic processes and morphologies: A numerical modeling study, *J. Geophys. Res. Earth Surf.*, *119*, 961–982, doi:10.1002/2013JF002965.

Cazanacli, D., C. Paola, and G. Parker (2002), Experimental steep, braided flow: Application to flooding risk on fans, *J. Hydraul. Eng.*, *128*, 322–330.

Davies, N. S., and M. R. Gibling (2011), Evolution of fixed-channel alluvial plains in response to Carboniferous vegetation, *Nat. Geosci.*, *4*(9), 629–633.

Day, J. W., G. P. Kemp, D. J. Reed, D. R. Cahoon, R. M. Boumans, J. M. Suhayda, and R. Gambrell (2011), Vegetation death and rapid loss of surface elevation in two contrasting Mississippi delta salt marshes: The role of sedimentation, autocompaction and sea-level rise, *Ecol. Eng.*, *37*(2), 229–240.

Edmonds, D. A., and R. L. Slingerland (2010), Significant effect of sediment cohesion on delta morphology, *Nat. Geosci.*, *3*(2), 105–109, doi:10.1038/Ngeo730.

Gacia, E., T. Granata, and C. Duarte (1999), An approach to measurement of particle flux and sediment retention within seagrass (Posidonia oceanica) meadows, *Aquat. Bot.*, *65*(1), 255–268.

Grabowski, R. C., I. G. Droppo, and G. Wharton (2011), Erodibility of cohesive sediment: The importance of sediment properties, *Earth Sci. Rev.*, *105*(3), 101–120.

Hamilton, P. B., K. Strom, and D. C. Hoyal (2013), Autogenic incision-backfilling cycles and lobe formation during the growth of alluvial fans with supercritical distributaries, *Sedimentology*, *60*(6), 1498–1525.

Hoyal, D. C. J. D., and B. A. Sheets (2009), Morphodynamic evolution of experimental cohesive deltas, *J. Geophys. Res.*, *114*, F02009, doi:10.1029/2007JF000882.

Jerolmack, D. J. (2009), Conceptual framework for assessing the response of delta channel networks to Holocene sea level rise, *Quat. Sci. Rev.*, *28*(17–18), 1786–1800, doi:10.1016/j.quascirev.2009.02.015.

Kim, W., and D. J. Jerolmack (2008), The pulse of calm fan deltas, *J. Geol.*, *116*(4), 315–330.

Kim, W., D. Mohrig, R. Twilley, C. Paola, and G. Parker (2009), Is it feasible to build new land in the Mississippi River Delta?, *Eos Trans. AGU*, *90*(42), 373–374.

Kostic, S., G. Parker, and J. G. Marr (2002), Role of turbidity currents in setting the forset slope of clinoforms prograding into standing fresh water, *J. Sediment. Res.*, *72*, 353–362.

Li, H., and S. Yang (2009), Trapping effect of tidal marsh vegetation on suspended sediment, Yangtze Delta, *J. Coast. Res.*, *25*, 915–924.

Martin, J., C. Paola, V. Abreu, J. Neal, and B. Sheets (2009a), Sequence stratigraphy of experimental strata under known conditions of differential subsidence and variable base level, *AAPG Bull.*, *93*(4), 503–533.

Martin, J., B. Sheets, C. Paola, and D. Hoyal (2009b), Influence of steady base-level rise on channel mobility, shoreline migration, and scaling properties of a cohesive experimental delta, *J. Geophys. Res.*, *114*, F03017, doi:10.1029/2008JF001142.

Muto, T. (2001), Shoreline autoretreat substantiated in flume experiments, *J. Sediment. Res.*, *71*(2), 246–254.

Muto, T., and R. J. Steel (1997), Principles of regression and transgression—The nature of the interplay between accommodation and sediment supply: Perspectives, *J. Sediment. Res.*, *67*(6).

Nardin, W., and D. A. Edmonds (2014), Optimum vegetation height and density for inorganic sedimentation in deltaic marshes, *Nat. Geosci.*, *7*(10), 722–726.

Nicholas, A., L. Clarke, and T. Quine (2009), A numerical modelling and experimental study of flow width dynamics on alluvial fans, *Earth Surf. Processes Landforms*, *34*(15), 1985–1993.

Nittrouer, J. A., J. Shaw, M. P. Lamb, and D. Mohrig (2012), Spatial and temporal trends for water-flow velocity and bed-material sediment transport in the lower Mississippi River, *Geol. Soc. Am. Bull.*, *124*(3–4), 400–414.

Ortiz, A. C., A. Ashton, and H. Nepf (2013), Mean and turbulent velocity fields near rigid and flexible plants and the implications for deposition, *J. Geophys. Res. Earth Surf.*, *118*, 2585–2599, doi:10.1002/2013JF002858.

Orton, G., and H. Reading (1993), Variability of deltaic processes in terms of sediment supply, with particular emphasis on grain size, *Sedimentology*, *40*(3), 475–512.

Paola, C., K. M. Straub, D. Mohrig, and L. Reinhardt (2009), The "unreasonable effectiveness" of stratigraphic and geomorphic experiments, *Earth Sci. Rev.*, *97*, 1–43.

Parker, G. (2004), 1D sediment transport morphodynamics with applications to rivers And turbidity currents, edited, St. Anthony Falls Laboratory, Univ. of Minnesota, Minneapolis.

Parker, G., T. Muto, Y. Akamatsu, W. E. Dietrich, and J. Lauer (2008), Unravelling the conundrum of river response to rising sea-level from laboratory to field. Part I: Laboratory experiments, *Sedimentology*, *55*(6), 1643–1655.

Peakall, J., P. J. Ashworth, and J. L. Best (2007), Meander-bend evolution, alluvial architecture, and the role of cohesion in sinuous river channels: A flume study, *J. Sediment. Res.*, *77*, 197–212.

Swenson, J. B., V. R. Voller, C. Paola, G. Parker, and J. G. Marr (2000), Fluvial-deltaic sedimentation: A generalized Stefan problem, *Eur. J. Appl. Math.*, *11*, 433–452.

Syvitski, J. P. (2005), The morphodynamics of deltas and their distributary channels, in *River Coastal Plain and Estuarine Morphodynamics: RCEM*, edited by G. Parker and M. H. García, pp. 143–150, Taylor and Francis, London.

Tal, M., P. Frey, W. Kim, E. Lajeunesse, A. Limare, and F. Metivier (2012), The use of imagery in laboratory experiments, in *Fluvial Remote Sensing for Science and Management*, edited by P. Carbonneau and H. Piegay, pp. 299–321, John Wiley, Oxford, U. K.

Van Dijk, M., G. Postma, and M. G. Kleinhans (2009), Autocyclic behaviour of fan deltas: An analogue experimental study, *Sedimentology*, *56*(5), 1569–1589.

Van Wagoner, J. C., R. M. Mitchum, K. M. Campion, and V. D. Rahmanian (1990), *Siliciclastic Sequence Stratigraphy in Well Logs, Cores, and Outcrops: Concepts for High-Resolution Correlation of Time and Facies*, AAPG Methods Explor. Ser., vol. 7, 55 pp., Tulsa, Okla.

Wickert, A. D., J. M. Martin, M. Tal, W. Kim, B. Sheets, and C. Paola (2013), River channel lateral mobility: Metrics, time scales, and controls, *J. Geophys. Res. Earth Surf.*, *118*, 396–412, doi:10.1029/2012JF002386.